Environmental risk in Northeast Brazil: estimation of burning areas in Coreaú River Basin, Ceará, Brazil

Ulisses Costa de Oliveira · Ernane Cortez Lima ·
Thomaz Willian Xavier de Figueiredo · Vanda de Claudino-Sales ⬛ ·
Carlos Eduardo Linhares Feitosa

Abstract This work aims to estimate the burned areas in the hydrographic basin of the Coreaú River, State of Ceará, north of Northeast Brazil, which has an area of 10,633.67 km^2, through the NOAA/ AVHRR satellite, between the years from 2010 and 2017. The data were acquired at the base of *INPE*, where they were tabulated and generated a vector file of points. A density map of the fire sources was elaborated, from which the burned areas were estimated in the watershed studied over the defined period of years. There were 1786 fire outbreaks, totaling an estimated accumulated area of 1187.66 km^2 of fires, which corresponds to 11.17% of the entire length of the hydrographic basin. The municipality of Mucambo presented a ratio of 40% of its territory comprised by the mapped fires. In relation to the conservation units, they mapped 795 hot spots in their perimeters.

Keywords Environmental hazard · Fire spots · Forest fires · Satellite mapping

Highlights
1. The conservation units located in the studied area were the most affected by the burned areas;
2. The Kernel density estimator proved to be efficient in analyzing the behavior of burned areas;
3. The occurrence of fires in the studied area is temporally and spatially well defined;
4. The methodology applied proved to be adequate to estimate areas of occurrence of burnt areas.

U. C. de Oliveira · T. W. X. de Figueiredo ·
V. de Claudino-Sales (✉)
UFC, Ceara, Brazil
e-mail: vcs@ufc.br

U. C. de Oliveira
e-mail: ucoliveira@msn.com

T. W. X. de Figueiredo
e-mail: thomwillian@gmail.com

E. C. Lima
UVA, Ceara, Brazil
e-mail: ernanecortez@hotmail.com

C. E. L. Feitosa
UFRGS, Rio Grande do Sul, Brazil
e-mail: eduardo.linhares@live.com

Introduction

Environmental risk is a term that means the possibility of occurrence of damage caused by environmental factors, which may be natural or caused by society (Aquino et al., 2017). Among the several types of environmental risks that exist today, those associated with forest fires are mentioned.

The literature on the mapping of forest fires covers several areas, from the use of remote sensing, through digital image processing, to the use of artificial intelligence methods (machine learning and deep learning). Currently, remote sensing techniques are the main sources of information, presenting a satisfactory cost–benefit ratio for mapping burnt areas on a regional, national, and even global scales. Data from medium and

low spatial resolution satellites have been used to map burning areas around the world. Examples include the Geostationary Operational Environmental Satellite — GOES, ATSR (along track scanning radiometer)/AATSR (advanced ATSR), National Oceanic and Atmospheric Administration — NOAA, Moderate Resolution Imaging Spectroradiometer Terra/Aqua — MODIS, Advanced Very-High-Resolution Radiometer — AVHRR, Satellite Pour l'Observation de la Terre — SPOT, Landsat, and China–Brazil Earth Resources Satellite — CBERS, Sentinel (Long et al., 2019; Giglio et al., 2013; Mallinis et al., 2017; Colson et al., 2018; Bar & Parida, 2020).

The use of remote sensing image processing tools can be carried out by means of several spectral indices, which are used both at the post-fire level, in the case of the unitemporal indices, and at the pre- and post-fire level, the bitemporal ones, aiming at conduct fire and burning gravity mapping using medium resolution images (Mallinis et al., 2017; Long et al., 2019; Bar et al., 2020; Colson et al., 2018; Arekhi et al., 2019, Fornacca et al., 2018; Hernandez-Leal et al., 2006). In addition to the indices, algorithms applied to images allow the detection of fire (Li et al., 2021) by means of aggregated classification to vegetation indices such as the region growth algorithm (Stroppiana et al., 2012) and spectral mixture analysis (Lima et al., 2019).

The fire risk forecasting models are addressed in several proposed works, providing tools for decision-makers to model environmental problems, using methodologies such as multicriteria decision analysis (MCDA) aided by geographic information systems (GIS) with the VIKOR and TOPSIS techniques (Sari, 2021), weighted linear combination (Çolak & Sunar, 2020; Jaiswal et al., 2002; Lein & Stump, 2009; Puri et al., 2011), neuro-fuzzy inference systems (ANFIS) (Moayedi et al., 2020), and linear regression (Eugenio et al., 2016).

In addition, machine learning techniques in recent years have been consolidated, gradually replacing traditional methods of mapping burn areas and risk maps, becoming a trend (Wang et al., 2019). Among the algorithms, some are more frequently used, such as convolutional neural networks (Barmpoutis et al., 2019; Liu et al., 2020; Wang et al., 2019), logistic regression (Toulouse et al., 2015), support vector machines (Liu et al., 2020; Zheng et al., 2020), and random forests (Belenguer-Plomer et al., 2019; Collins et al., 2018).

Forest fires are a major cause of damage to forest ecosystems. They stand out because they considerably compromise the stability of the process of environmental resilience, causing serious risks to the sustainability of the environment. Several factors are directly related to the occurrence of forest fires, such as the composition of the combustible material in the area, climatic variables, relief, declivity, use, and occupation, among others.

Fires are an annual occurrence in many parts of the world, causing severe damage to natural and built environments (Veeraswamy et al., 2018). In regions of economic development, the pressures that forest areas suffer due to the need for new areas destined for agricultural activities have considerably increased the number of fires and the extension of areas burned due to the misuse of fire as an agricultural tool (Salinero & Isabel, 2004). In addition, common causes are the action of arsonists, hunters, anglers, and the release of balloons, among others (Alves & Nóbrega, 2011).

Whether natural or anthropogenic, the effects of fires can be catastrophic and have the power to devastate thousands of hectares of vegetation, as well as to suppress human and animal life year by year. Fires also alter the availability of natural resources, with a consequent impact on the daily life of neighboring communities (Tardivo et al., 2017). For this reason, the issue of forest fires is a topic that has been extensively researched by the scientific community, so that several researchers have sought to understand the causes, effects, and ways to comprehend the behavior of this environmental risk (e.g. Veeraswamy et al., 2018; Zheng et al., 2017; White, Oliveira and Ribeiro 2017; Torres et al., 2017; Zheng et al., 2016).

Within this problem, some areas are much more vulnerable to the occurrence of fires among which stands out the Brazilian semi-arid region, that is characterized by the spatial and temporal irregularity of the rainfall distribution, as well as the characteristics of the vegetation in the dry season. When all these aspects are related to the high-temperature characteristics of the region for most of the year and to the practice of intensive family farming, besides other aspects (physical, anthropic, such as the processes of desertification and global warming), the generalized occurrence of forest fires becomes even more intense.

In fact, in the Brazilian semi-arid, particularly in the Northeast of the Ceará, it is the population's cultural practice to carry out the removal of vegetation, aiming at the alternative use of the soil for agricultural activities and vegetal extraction. In addition, agricultural production, if practiced incorrectly, can cause damage to the environment, contributing to the degradation of the physical and biotic means. The vegetation of the Caatinga serves as fuel for industrial

activities, which promotes intensification in the processes of vegetable degradation, influencing from the temperature to the water availability, therefore requiring a monitoring of vegetation and soil management conditions in the region (Oliveira & Oliveira, 2017).

In the context of Ceará, the issue of lack of water in the watersheds further accentuates this problem. Thus, forest fires, to the extent they compromise the availability of vegetation, directly interfere with the question of water resources.

In order to understand these problems, this paper presents an estimate of burned areas in the basin of Coreaú river, located in the northwest of the State of Ceará, during the years 2010 to 2017. It was decided to work the category "watershed" as an element of analysis, because it is an important space unit for the environmental management focused on the conservation of natural resources. At that time, the degree of degradation resulting from inappropriate practices of use/occupation of natural resources inserted in the basin was also verified, although this is not the focus of the discussion.

The use of the hydrographic basin concept as a study and management unit with the aim of conserving natural resources, in line with the concept of Sustainable Development, sought to achieve three basic objectives, namely, social, economic, and environmental equity and also sustainability, as indicated by

Pires et al. (2008). These goals show the long-term interdependence of economic and social development with the protection of the physical environment, making clear the concern with the degradation and maintenance of the systems and subsystems present in the watershed. In effect, the consequent management of the watershed occurs when "environmental management uses the river basin as a unit of planning and intervention" (Lima, 2012).

Characterization of the study area

The study area comprises the Coreaú River Basin (CRB) located between the geographic coordinates 41°27′ and 40°10′ west latitude and 2°44′ and 4°10′ south longitude (Fig. 1). According to COGERH (2010), the basin is located in the northwestern portion of the State of Ceará, geographically limited to the south by the Poti-Longá and Acaraú basins, to the west by the State of Piauí, to the east by the Acaraú basin and to the north by the Atlantic Ocean.

The basin has a coastline extension of approximately 130 km, represented in Fig. 1, being composed by the drained area of the Coreaú river and its tributaries, as well as sub-basins formed by the rivers Timonha, Tapuio, Pesqueiro, Jaguarapari, Corrente Laranja, Lago Seco, Mourão, Forquilha, Poeira, and

Fig. 1 Location of the watershed of the Coreaú river, Northeast of Brazil. Source: elaborated by the authors
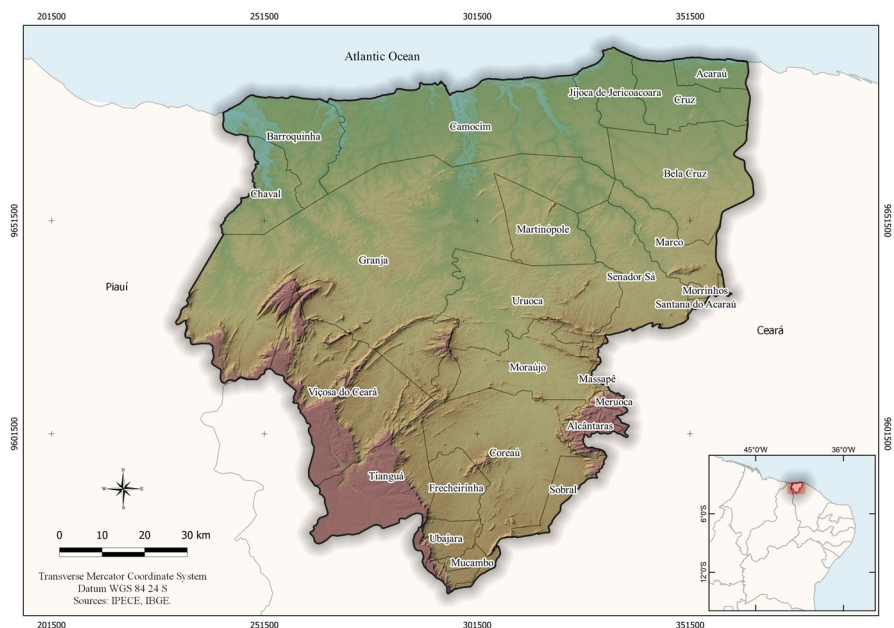
Prata. This group comprises 10,633.67 km² of area, corresponding to 7% of the territory of Ceará, fully covering the area of 10 counties and, partially, of another 14 counties located nearby.

The choice of the hydrographic basin of the Coreaú River was due to the heterogeneity of relief features from the point of view of geomorphological importance, which includes the Ibiapaba Plateau to the west, the Meruoca Residual Massif to the southeast, the Sertaneja Surface, to scattered river plains throughout the area and to the north the pre-coastal plain and the coastal plain, the latter on the coast with the Atlantic Ocean.

Materials and methods

The detection of fires and forest fires through satellites is a relatively old technology, initiated in the 1980s. In general, globally, the National Oceanic and Atmospheric Administration (NOAA), Advanced Very High-Resolution Radiometer (AVHRR), and the Moderate Resolution Imaging Spectroradiometer (MODIS) satellites are the most used, being the main tools for detecting forest fires (Wang et al., 2012).

According to Kazmierczak (2015), the identification of forest fires by means of satellite images occurs through the detection of heat sources by the temperature difference between the targets photographed on the Earth's surface. The satellite sensor measures the thermal radiance of the imaged area in a given passage and converts it to a brightness temperature, also called radiance temperature, and then calculates the coordinates of the focus of the forest fire.

Satellites that detect biomass fire outbreaks or "heat outbreaks" generate a great volume of data. Despite the technological progress related to the digital processing of this information, a series of difficulties persist, especially concerning data validation since several errors can occur during the collection process due to false detections. According to Koltunov et al. (2012), the difficulties in detecting fires are related to validation methodologies that continue to pose huge challenges regarding the correction of false positives, i.e., the detection of fires that did not in fact take place. Hence, it is of utmost importance to use tools that allow the evaluation of data to remove false positives,

filter, and retain data with low precision information on fires.

Geoprocessing tools provide considerable gains due to their low cost, relative ease of use, and coverage of wide areas such as large river basins whose water potential is closely related to the vegetation.

Obtaining the data

The data of this work were acquired in the base of the National Institute of Space Research (INPE), in vector file in text format, available at <http://www.inpe.br/queimadas/bdqueimadas>.

The collected data were tabulated, and then, a comma-separated value (.csv) file was generated and subsequently imported into the GIS environment using QGIS, version 2.14 Essen. Next, a vector file of points in shapefile format was created, with coordinate reference system defined in WGS 84/UTM zone 24S.

Thus, it was generated a cloud of points containing information per year from the burning outbreaks in the watershed of the Coreaú river. These were the basis for generating the data analyzed in the present work.

To estimate the burnt areas, the methodology developed by Setzer and Pereira (1991) apud Kazmierczak (2015) was applied to obtain an approximate burn area, whose formula (1) determines the burnt area estimate based on the number of heats identified in NOAA Images:

$$BA = \left(\frac{Number\ of\ Focus}{1.5}\right) \times 0.63 \times 1.21 \qquad (1)$$

where BA represents the burned area in km², 1.5 the constant relative to the duration of the burning (average number of days of burning), 0.63 the burned area factor, and 1.21 km² to the NOAA/AVHRR pixel area. In the case of the burned area, Setzer and Pereira (1991), published in Institute for Applied Economic Research — IPEA (2002), justifying the factor of the burned area, have stated that, in many cases, the area actually burned is much smaller than the area of the pixel. According to the authors, as a matter of fact, the satellite records the occurrence of a heat source because of its high temperature, being that the focus may cover a small area or represent the whole area of the pixel.

In this context, it is important to consider that a forest fire is any fire that is out of control that affects any form of vegetation, whether man-made (intentional or due to neglect) or caused naturally (lightning) and that can cause damage to humans or the environment (ICMBIO, 2010). To Lacerda (2013), a forest fire is any fire that is out of control that affects any form of vegetation triggered by natural causes (lightning) or brought about accidentally (neglect) or intentionally (by arsonists). A heat outbreak, in turn, is data captured by a monitoring satellite that is 700 to 900 km above the Earth. The satellite sensors register temperatures above 47 °C. A fire or occurrence can lead to one or several heat outbreaks, depending on the extension of the line of fire. A heat outbreak is not necessarily a fire outbreak or a fire (Lacerda, 2013).

To elaborate the map of the density of heat sources, the Kernel density estimator was used, contained in the QGIS heat map tool. From the heat map function, a matrix file and output as a result of the sum of the stacking of "n," and other circular raster radius "h" for each point of the input data according to the formula (1) are shown below:

$$\widehat{f}_h(x) = \frac{1}{nh} \sum_{i=1}^{n} K\left(\frac{x - X_i}{h}\right) \tag{2}$$

in which K = kernel function, h = search radius, x = position of the center of each cell of the output raster, Xi = position of "i" point from the centroid of each polygon, and n = total number of environmental infractions.

The density estimator Kernel draws a circular neighborhood around each sample point, corresponding to the radius of influence, and then a mathematical function of 1 is applied at the point position to 0 at the neighborhood boundary. The value for the cell is the sum of the overlapping kernel values and divided by the area of each search radius (Silverman, 1986).

In order to identify the regions of concentration of fires, the classification was used: null (0 foci), very low (0.1 to 15 foci), low (16 to 30 foci), medium (31 to 40 foci), high (41 to 60 foci), and very high (> 60 foci). For this map, all the fire outbreaks mapped in the basin by the satellites AQUA, GOES, MSG, NOAA, NPP, and TERRA were considered.

Finally, after preparing the map containing the regions of thermal focus density, the raster data generated based on the rendering of the image band in the false color single band option were reclassified, categorizing them into six classes, as described in the previous paragraph.

To analyze the validity of the results estimated through the model used in the present study, mapping of fire scars by means of visual interpretation with the delimitation of regions of interest based on fire scars is carried out. For mapping of scars, images 133 s of the Landsat 8 satellite of the United States Geological Survey (USGS) — http://landsat.usgs.gov/, OLI sensors (Operational Land Imager), and TIRS (Thermal Infrared Sensor), Orbit 218, points 062 and 063 with a spatial resolution of 30 m, were used. Images with up to 20% cloud coverage were used; the image orbit/point and data are cited in Table 1.

Mapping of burned areas was done based on the following stages: preprocessing of the LandSat8 images (correction, mosaic, normalized difference vegetation index — NDVI and image difference of NDVIs), semiautomatic segmentation, and classification by means of the region growing algorithm, refinement, and vectorization. In addition, vectorial and matricial editing was carried out to minimize classification errors. The results obtained required editing to correct possible errors that occurred during automatic processing. To do this, the lines of the classified map polygons, represented vectorially, were superimposed onto the colored composition of the original images (RGB 753) and important additional information available for the studied area. The resulting data were used as a reference for quantitative analysis of the burned areas estimated by formula (1).

After the data bank with information on fires was created, a correlation analysis among data was done

Table 1 Orbit, point, and data of images used

Orbit/point	Date of images
218/062	09/26/2013; 08/12/2014; 10/15/2014; 08/31/2015; 11/19/2015; 08/02/2016; 09/02/2016; 11/06/2016; 09/08/2017; 10/23/2017
218/063	09/26/2013; 08/12/2014; 10/15/2014; 08/31/2015; 11/19/2015; 02/08/2016; 09/02/2016; 11/06/2016; 09/08/2017; 10/23/2017

by using Pearson's correlation coefficient which, according to Toledo and Ovalee (1995a), indicates the match between two series of measurements, measuring the degree of linear relation between two quantitative variables, varying between -1 and 1. The closer it is to 1 or -1, the stronger the linear association between two variables, which can be an inverse perfect linear relation (approximate values to -1) or a positive perfect linear relation, when values are approximate to 1. Zero (0) value indicates that there is no linear relation. The coefficient is calculated with the following equation:

$$R = \frac{\sum_{i=1}^{n}(x_i - \overline{x})(y_i - \overline{y})}{\sqrt{\sum_{i=1}^{n}(x_i - \overline{x})^2 \sum_{i=1}^{n}(y_i - \overline{y})^2}} \tag{3}$$

where R is the correlation coefficient, x_i are values of variable x in a sample, $\overline{x}$ is the average value of variable x, y_i are values of variable y in the sample, and $\overline{y}$ is the average value of variable y. For regression analysis, the coefficient of adjusted determination (denoted as R^2) of the following equation (Kvålseth, 1985):

$$R^2 = 1 - \frac{n-1}{n-p}\frac{\sum_{i=1}^{n}(x_i - \widehat{x}_i)^2}{\sum_{i=1}^{n}(x_i - \widehat{x})^2} \tag{4}$$

where n is the number of samples, p is the number of parameters, x_i is the umpteenth original value, and $\widehat{x}_i$ is the umpteenth estimated value. Test statistics was adopted for the coefficients obtained in the regression model at a significance level of 0.01. Thus, the null hypothesis for the test statistics used in this study is that the coefficients are equal to zero (H_0 $\rho=0$). When the value of p is smaller than the significance level, the null hypothesis is rejected (H_0 $\rho \neq 0$), and the coefficient will be considered statistically significant. The same data validation approach was used in several papers that dealt with the estimate of fire areas (Li et al., 2021; Arekhi et al., 2019; Long et al., 2019; Mallinis et al., 2017).

For the analysis of the difference among the values analyzed, a data distribution evaluation was done, as well as if the differences among values of the areas estimated by images and by formula (1) were significantly different or not, checking to see if there is evidence to believe that the values in a group are greater than those in another group.

Results and discussion

After the treatment of the acquired data and their interpretation, the occurrence of 1786 fires has been found, totaling an estimated cumulative area of 1187.66 km^2 of fires, which corresponds to 11.17% of the whole length of the basin analyzed the years studied.

The evolution of the number of fires per month over the years studied is shown in Fig. 2. The dominant climatic dynamics in Ceará State is a factor that conditions the predominance of burnt outbreaks in the months of August to December in all years, since at this time, the preparation of the land for the planting before the rainy season occurs, which in the State occurs between the months of February to May.

The month of December presented the highest amount accumulated in the analyzed period, totaling 1033 hot spots, followed by November and October, with 762 and 233 outbreaks, respectively. The months of November and December presented a number of outbreaks above the annual average, which was 292 fires. In the months of February to June, when there were rains in Ceará State, there were almost no hot spots, evidencing a temporal pattern of soil use in the region studied.

Regarding the estimation of deforested areas, these are directly proportional to the number of heat sources. Therefore, the highest numbers of deforested areas are concentrated in the months when there were more outbreaks. The month of December totaled 524.97 km^2 of burned area, followed by November (387.25 km^2) and October (118.41 km^2), according to Table 2.
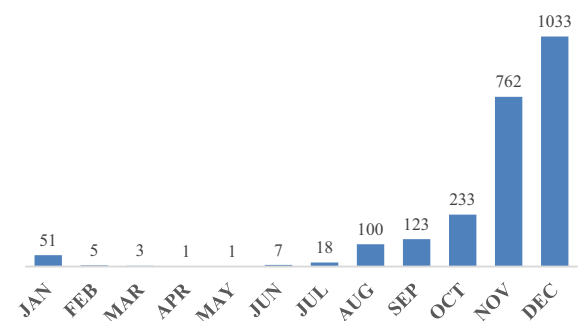
Fig. 2 Number of heat sources accumulated per month in the years of 2010 to 2017. Source: elaborated by the authors

Table 2 Quantitative analysis of burned areas (km^2) per month and year in the watershed of the Coreaú river, from 2010 to 2017. Source: elaborated by the authors

Month	Year								Monthly total
	2010	2011	2012	2013	2014	2015	2016	2017	
Jan	3.56	0.00	6.10	1.02	3.56	3.05	1.52	7.11	25.92
Feb	1.52	0.00	1.02	0.00	0.00	0.00	0.00	0.00	2.54
Mar	1.02	0.51	0.00	0.00	0.00	0.00	0.00	0.00	1.53
Apr	0.51	0.00	0.00	0.00	0.00	0.00	0.00	0.00	0.51
May	0.51	0.00	0.00	0.00	0.00	0.00	0.00	0.00	0.51
Jun	1.02	0.00	0.00	0.00	0.00	0.00	1.52	1.02	3.56
Jul	2.03	0.00	0.00	0.00	0.51	1.52	5.08	0.00	9.15
Aug	0.00	0.51	3.05	0.00	2.03	1.52	39.13	4.57	50.82
Sep	3.05	5.08	4.07	1.02	2.54	3.56	13.21	29.98	62.51
Oct	3.05	6.61	9.66	7.11	6.10	21.34	46.75	17.79	118.41
Nov	4.57	13.21	5.59	67.59	66.07	40.66	76.23	113.33	387.25
Dec	5.08	20.84	6.61	104.18	60.98	48.79	128.07	150.43	524.97
Total annual	25.92	46.75	36.08	180.92	141.79	120.44	311.53	324.23	1187.66

Still observing Table 2, there are low values of burned areas in the months from February to June, according to the court wintry period, when the fires have already occurred and the plantations were carried out (Table 3).

Table 3 Quantitative analysis of heat sources, burned areas, and percentage relations with the areas of the counties inserted in the watershed of the Coreaú river in the years of 2010 to 2017. Source: elaborated by the authors

Counties	Number of outbreaks	Burn area (km^2)	Of burned area in the territory of counties
Alcântaras	10	5.08	4%
Meruoca	14	7.11	5%
Frecheirinha	59	29.98	17%
Mucambo	149	75.72	40%
Jijoca de Jericoacoara	10	5.08	3%
Chaval	94	47.77	17%
Martinópole	11	5.59	2%
Cruz	29	14.74	4%
Barroquinha	39	19.82	5%
Morrinhos	25	12.71	3%
Ibiapina	44	22.36	5%
Moraújo	45	22.87	6%
Ubajara	56	28.46	7%
Senador Sá	22	11.18	3%
Marco	49	24.90	4%
Uruoca	107	54.38	8%
Coreaú	159	80.80	10%
Bela Cruz	82	41.67	5%
Acaraú	64	32.52	4%
Tianguá	233	118.41	13%
Camocim	85	43.20	4%
Viçosa do Ceará	375	190,58	15%
Sobral	202	102.66	5%
Granja	374	190.07	7%

Fig. 3 Density of heat sources accumulated between the years of 2010 and 2017 in the watershed of Coreaú river. Source: elaborated by the authors
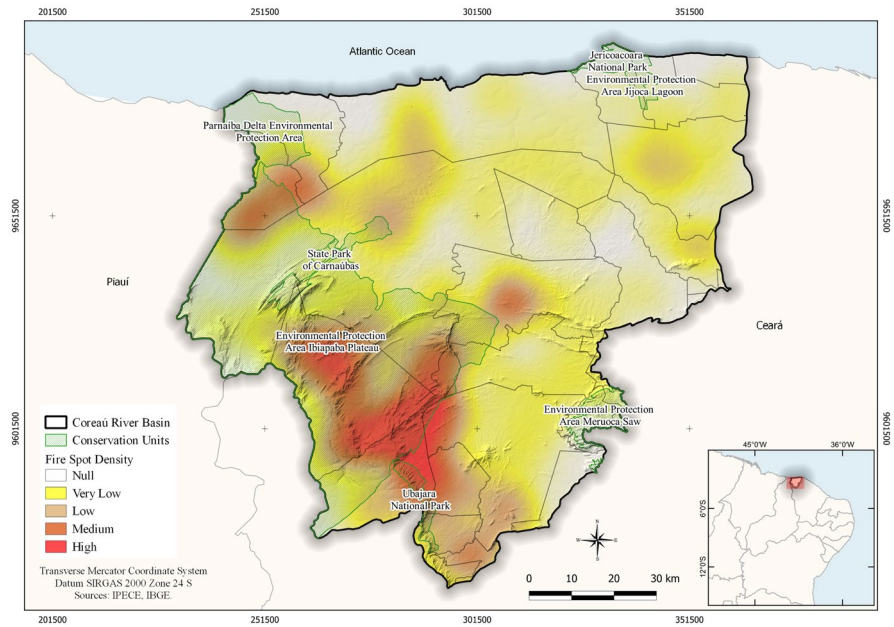
In the context of the 24 municipalities that are part of the basin, a comparison was made between the estimated areas of fires in relation to the territory of the municipality as a whole, not just its portion inserted in the basin, since the data provided cover its entire area. According to chart 3, the county of Mucambo, in the accumulated years analyzed, presented a ratio of 40% of its territory covered by the mapped fires, making 75.72 km^2 over an area of 190.54 km^2.

In addition to Mucambo, the counties of Frecheirinha (17%), Chaval (17%), Viçosa do Ceará (15%), Tianguá (13%), and Coreaú (10%) presented a high percentage of their territories with burned areas mapped.

With the increasing occupation and conversion of the Caatinga into agricultural areas, the conservation units (UC — Unidades de Conservação) located in this biome have been constantly impacted by the continuous action of forest fires (Medeiros, 2002).

In relation to these units, in the context of the CRB, these total seven units (Fig. 3), three of integral protection and four of sustainable use. The state UCs are the Environmental Protection Area (Área de Proteção Ambiental — APA) of Lagoa de Jijoca and Carnaúbas State Park. The other UCs are managed by the federation, which are the APA Delta do Parnaíba, APA Serra da Ibiapaba, APA Serra da Meruoca, National Park of Jericoacoara, and Ubajara National Park. Together, the seven UCs, in the portions inserted in the territory of the hydrographic basin of the Coreaú, total an area of 3311.19 km^2, representing 31% of the basin area.

Over the study period, as conservation units mapped 795 hot spots in their perimeters, 90% of which occurred in APA Serra da Ibiapaba, mapping 719 hot spots, representing an estimated burned area of 365.40 km^2. This frame can be explained, in part, by the uses that occur in the Ibiapaba Plateau region, quite geared to agricultural activities, through indiscriminate deforestation and the use of fires, which can lead to soil depletion, as well as the significant reduction and impoverishment of biodiversity.

Table 4 Data on burn areas (km^2) obtained by means of satellite image analysis (reference) and estimated by formula 1 (estimate)

Date	Reference (km^2)	Estimated (km^2)	Difference (km^2)
Aug/2013	7.11	6.29	0.82
Aug/2014	7.15	5.08	2.07
Oct/2014	4.17	6.1	− 1.93
Aug/2015	4.9	3.4	1.5
Nov/2015	44.9	40.66	4.24
Aug/2016	4.71	5.08	− 0.37
Sep/2016	32.72	39.13	− 6.41
Nov/2016	67.84	59.96	7.88
Sep/2017	3.83	29.98	− 26.15
Oct/2017	28.24	17.79	10.45

Fig. 4 Relation between estimated fire scar area (axis y) and areas obtained through images (axis x)
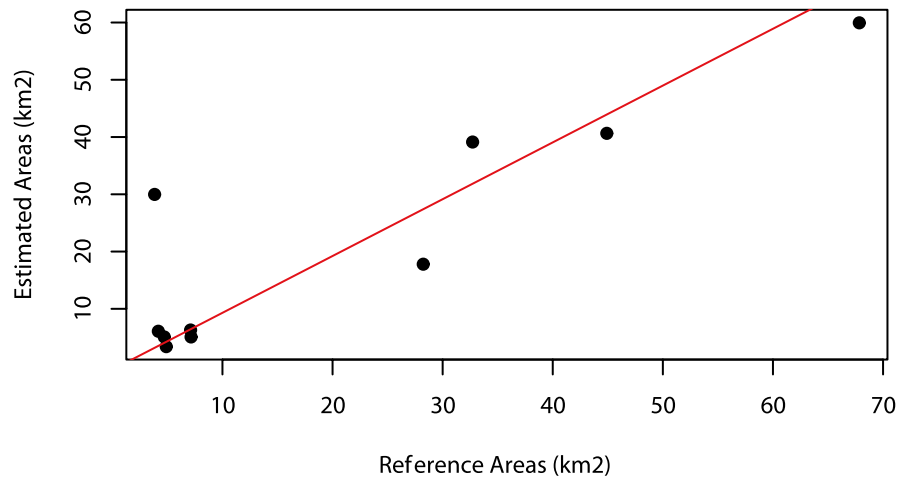
In relation to the spatial distribution of heat sources in the studied basin, Fig. 3 presents the densities accumulated in the studied years, obtained through the Kernel density algorithm. The density classes of the outbreaks were distributed according to the results of the operations performed through the software.

Figure 3 shows that the highest concentrations of heat sources in the basin are located in the northwest and southwest portion of the area, in the perimeters of the APA Ibiapaba Serra and Ubajara National Park, which indicates the intense anthropic influence in the conservation. The outbreaks covered forest areas and the most impacted typologies were the Pluvial-Nebular Tropical Subperenifólia Rainforest, the Tropical Pluvial Sub-deciduous Forest, and the Thorny Deciduous Forest.

As for the validation of estimated data, Fig. 4 shows the dispersion graphics among measurements made by surveys done with satellite images and those estimated by formula (1). Based on the results of test statistics, the coefficients and constants of the regression function are statistically significant ($P < 0,001$ in $\alpha = 0.01$). Data presents a correlation coefficient in the order of 0.89 which evinces a positive linear correlation among variables. Coefficient R^2 presents a value of 0.7931 with P-value of 0.000549, meaning that these values are statistically significant.

For the analysis of data distribution, the Shapiro–Wilk test was applied, presenting a P-value < 0.05, indicating the non-normality of data distribution. Because of this,

and considering the size of the samples ($n = 10$), the Mann–Whitney test was applied, presenting a statistic of U = 46 and P-value = 0.762, evincing that there is no statistical difference among the compared data.

Thus, one can say that, statistically speaking, based on the data analysis presented in Table 4, the values of areas estimated by formula (1) do not show significant differences in relation to the data taken from satellite image interpretation used as a validation parameter.

Conclusions

The situations analyzed in this article allow us to draw the following conclusions:

- The highest concentrations of forest fires are located inside the conservation units APA Serra da Ibiapaba, APA Delta do Parnaíba, and Ubajara National Park, located in the Ibiapaba Plateau, which can be explained by a greater propensity of these areas for agricultural activities;
- The years of 2016 and 2017 presented results well above the average of the analyzed period, which requires a deepening of the policies to combat the indiscriminate use of fire in the studied region, considering that these practices directly influence the water availability of the basin;

- The data provided by *INPE* for the NOAA/ AVHRR satellite allowed to estimate the area burned in the basin, which totaled 1187.66 km^2, corresponding to 11.17% of all the extension of the hydrographic basin analyzed from the long years of the studied years;

- Through the kernel density estimator, it was possible to analyze the behavior of the heat sources, generating qualitative information about the hydrographic basin of the Coreaú river during the studied period. It is important to deepen this type of work, in the sense of crossing information with databases of land use, plant cover, and geoenvironmental units (*unidades geoambientais*), among others.

It is emphasized that it is necessary to implement public policies aimed at systematic and periodic monitoring throughout the territory of the hydrographic basin, both in combating degrading practices through the use of indiscriminate fire and in understanding the dynamics of these practices, thus offering measures that can minimize them throughout the territory of the basin.

Finally, it is considered that the data above indicate that there is an urgent need for government and society to fight forest fires, considering the direct relationship between vegetation and the availability of water, therefore with the quality of life of the populations of the Northeast of Brazil. Only in this way will it be possible to effectively manage the environmental risk represented by forest fires to which the environment and the population are subject or may still be subject.

References

Alves, K. M. A. S., & Nóbrega, R. S. (2011). Uso de dados climáticos para análise espacial de risco de incêndio florestal. *Mercator, Fortaleza, 10*(22), 209–219.

ANA / BANCO MUNDIAL / PROÁGUA NACIONAL / COGERH. (2010). *Plano de Gerenciamento das Águas da Bacia do Coreaú. Fase 1: Estudos Básicos e Diagnóstico.* Fortaleza – CE.

Arekhi, M., Goksel, C., Balik Sanli, F., & Senel, G. (2019). Comparative evaluation of the spectral and spatial consistency of Sentinel-2 and Landsat-8 OLI Data for Igneada Longos Forest. *ISPRS International Journal of Geo-Information., 8*(2), 56. https://doi.org/10.3390/ijgi8020056.

Aquino, AR, Paletta, FC, Almeida, JR. (Orgs) (2017). *Risco Ambiental.* São Paulo: Edgard Blucher.

Instituto de Pesquisa Econômica Aplicada (IPEA) . (2002). *O custo econômico do fogo na Amazônia.* Texto para discussão n. 912. Rio de Janeiro.

Bar, S., Parida, B. R., & Pandey, A. C. (2020). Landsat-8 and Sentinel-2 based forest fire burn area mapping using machine learning algorithms on GEE cloud platform over Uttarakhand, Western Himalaya *Remote Sensing Applications*: *Society and Environment, 18,* 100324 https://doi.org/10.1016/j.rsase.2020.100324.

Barmpoutis, P., Dimitropoulos, K., Kaza, K., & Grammalidis, N. (2019).Fire detection from images using faster R-CNN and multidimensional texture analysis. *ICASSP 2019 - 2019 IEEE International Conference on Acoustics, Speech and Signal Processing (ICASSP).* Published online May 2019. https://doi.org/10.1109/ICASSP.2019.8682647.

Belenguer-Plomer, M. A., Tanase, M. A., Fernandez-Carrillo, A., & Chuvieco, E. (2019) Burned area detection and mapping using Sentinel-1 backscatter coefficient and thermal anomalies *Remote Sensing of Environment, 233,* 111345 https://doi.org/10.1016/j.rse.2019.111345.

Çolak, E., Sunar, F. (2020) Evaluation of forest fire risk in the Mediterranean Turkish forests: A case study of Menderes region, *Izmir International Journal of Disaster Risk Reduction,* 45, 101479 https://doi.org/10.1016/j.ijdrr.2020.101479.

Collins, L., Griffioen, P., Newell, G., & Mellor, A. (2018). The utility of random forests for wildfire severity mapping. *Remote Sensing of Environment., 216*, 374–384. https://doi.org/10.1016/j.rse.2018.07.005.

Colson, D., Petropoulos, G. P., & Ferentinos, K. P. (2018). Exploring the potential of Sentinels-1 & 2 of the Copernicus mission in support of rapid and cost-effective wildfire assessment. *International Journal of Applied Earth Observation and Geoinformation., 73*, 262–276. https://doi.org/10.1016/j.jag.2018.06.011.

Eugenio, F. C., dos Santos, A. R., Fiedler, N. C. et al. (2016). Applying GIS to develop a model for forest fire risk: A case study in Espírito Santo. *Brazil. Journal of Environmental Management., 173,* 65–71. https://doi.org/10.1016/j.jenvman.2016.02.021.

Fornacca, D., Ren, G., & Xiao, W. (2018). Evaluating the best spectral indices for the detection of burn scars at several post-fire dates in a mountainous region of Northwest Yunnan, China. *Remote Sensing., 10*(8), 1196. https://doi.org/10.3390/rs10081196.

Giglio, L., Randerson, J. T., & van der Werf, G. R. (2013). Analysis of daily, monthly, and annual burned area using the fourth-generation global fire emissions database (GFED4). *Journal of Geophysical Research: Biogeosciences., 118*(1), 317–328. https://doi.org/10.1002/jgrg.20042.

Hernandez-Leal, P. A., Arbelo, M., & Gonzalez-Calvo, A. (2006). Fire risk assessment using satellite data. *Advances*

in Space Research., *37*(4), 741–746. https://doi.org/10.1016/j.asr.2004.12.053.

ICMBIO. (2010). *Manual para Formação de Brigadista de Prevenção e Combate aos Incêndios Florestais.* [s.l.]: , [s.d.]. Available at: <https://www.icmbio.gov.br/portal/images/stories/servicos/sejaumbrigadista.pdf>. Accessed in 25 Apr 2021.

Jaiswal, R. K., Mukherjee, S., Raju, K. D., & Saxena, R. (2002). Forest fire risk zone mapping from satellite imagery and GIS. *International Journal of Applied Earth Observation and Geoinformation.*, *4*(1), 1–10. https://doi.org/10.1016/s0303-2434(02)00006-5.

Kazmierczak, M. L. (2015). Sensoriamento Remoto para Incêndios Florestais. *In*: Sausen, TM, Lacruz, MSP (Org.). (2015). *Sensoriamento Remoto para Desastres.* São Paulo: Oficina de Textos.

Koltunov, A., Ustin, S. L., & Prins, E. M. (2012). On timeliness and accuracy of wildfire detection by the GOES WF-ABBA algorithm over California during the 2006 fire season.*Remote sensing of environment*, *127*, 194-209.

Kvålseth, T. O. (1985). Cautionary note about R^2. *Am. Statist.*, *39*(4), 279–285.

Lein, J. K., & Stump, N. I. (2009). Assessing wildfire potential within the wildland–urban interface: A southeastern Ohio example. *Applied Geography.*, *29*(1), 21–34. https://doi.org/10.1016/j.apgeog.2008.06.002.

Lacerda, F. (2013). *Prevenção e monitoramento de incêndios florestais em terras indígenas: Programa de capacitação em proteção territorial.* FUNAI – Fundação nacional do Índio. Brasília: FUNAI/GIZ, 2013. 96 p. ISBN: 978–85–7546–042–9. Available at <http://www.funai.gov.br/arquivos/conteudo/cgmt/pdf.> Accessed in 25 Apr 2021.

Li, P., Yang, Y., Zhao, W., & Zhang, M. (2021). Evaluation of image fire detection algorithms based on image complexity *Fire Safety Journal*, *121,* 103306 https://doi.org/10.1016/j.firesaf.2021.103306.

Lima, EC. (2012). *Planejamento ambiental como subsídio para gestão ambiental da bacia de drenagem do açude Paulo Sarasate Varjota – Ceará.* Fortaleza. 201f. Tese (Doutorado em geografia) – Universidade Federal do Ceará, UFC.

Lima, T. A., Beuchle, R., Langner, A., Grecchi, R. C., Griess, V. C., & Achard, F. (2019). Comparing Sentinel-2 MSI and Landsat 8 OLI imagery for monitoring selective logging in the Brazilian Amazon. *Remote Sensing.*, *11*(8), 961. https://doi.org/10.3390/rs11080961.

Liu, Z., Zhang, K., Wang, C., & Huang, S. (2020). Research on the identification method for the forest fire based on deep learning *Optik, 223,* 165491 https://doi.org/10.1016/j.ijleo.2020.165491.

Long, T., Zhang, Z., He, G. et al. (2019). 30 m Resolution global annual burned area mapping based on Landsat Images and Google Earth Engine. *Remote Sensing.*, *11*(5), 489. https://doi.org/10.3390/rs11050489.

Malinis, G., Mitsopoulos, I., Chrysafi, I. (2018). Evaluating and comparing Sentinel 2A and Landsat-8 Operational Land Imager (OLI) spectral indices for estimating fire severity in a Mediterranean pine ecosystem of Greece. *GIScience & Remote Sensing*. Published 2018. Accessed 16 Mar2021. https://www.tandfonline.com/doi/full/ https://doi.org/10.1080/15481603.2017.1354803.

Medeiros, M. B. (2002). *Efeitos do fogo nos padrões de rebrotamento em plantas lenhosas, em campo sujo.* Tese (Doutorado em Engenharia Florestal), p. 122. Universidade de Brasília, Brasília.

Moayedi, H., Mehrabi, M., Bui, D. T., Pradhan, B., & Foong, L. K. (2020). Fuzzy-metaheuristic ensembles for spatial assessment of forest fire susceptibility. *Journal of environmental management*, *260*, 109867. https://doi.org/10.1016/j.jenvman.2019.109867.

Oliveira, U. C., & de Oliveira, P. S. (2017). Mapas de Kernel como Subsídio à Gestão Ambiental: Análise dos Focos de Calor na Bacia Hidrográfica do Rio Acaraú, Ceará, nos Anos 2010 a 2015 Espaço Aberto, PPGG - UFRJ, Rio De Janeiro 7(1)87-99.

Pires, J. S. R., Santos, J. E., Del Prette, M. E. (2008). A utilização do conceito de bacia hidrográfica para a conservação dos recursos naturais. *In*: Schiavetti, A and Camargo, A.F.M. (Orgs.). (2008). *Conceitos de bacias hidrográficas:* teorias e aplicações. Ilhéus, BA. Editus.

Puri, K., Areendran, G., Raj, K., Mazumdar, S., & Joshi, P. K. (2011). Forest fire risk assessment in parts of Northeast India using geospatial tools. *Journal of Forestry Research.*, *22*(4), 641–647. https://doi.org/10.1007/s11676-011-0206-4.

Salinero, E. C, Isabel, M. P. M. (2004). *Nuevas Tecnologías para la estimación del riesgo de incendios forestales.* Editorial CSIC – CSIC Press. Madrid, n. 109, 194.

Sari, F. (2021) Forest fire susceptibility mapping via multicriteria decision analysis techniques for Mugla, Turkey: A comparative analysis of VIKOR and TOPSIS *Forest Ecology and Management,* 480, 118644 https://doi.org/10.1016/j.foreco.2020.118644.

Setzer, A., & Pereira, M. (1991). Amazônia biomass burning in 1987 and an estimate on their tropospheric emissions. *Ambio, 20*(1), 19–22.

Silverman, B. W. (1986). Density estimation for statistics and data analysis. *Monographs on Statistics and Applied Probability*, London: Chapman and Hall. https://ned.ipac.caltech.edu/level5/March02/Silverman/paper.pdf.

Stroppiana, D., Bordogna, G., Carrara, P., Boschetti, M., Boschetti, L., & Brivio, P. A. (2012). A method for extracting burned areas from Landsat TM/ETM+ images by soft aggregation of multiple Spectral Indices and a region growing algorithm. *ISPRS Journal of Photogrammetry and Remote Sensing.*, *69*, 88–102. https://doi.org/10.1016/j.isprsjprs.2012.03.001.

Tardivo, M. L., Caymes-Scutari, P., Bianchini, G., Méndez-Garabetti, M., Cencerrado, A., & Cortés, A. (2017). A comparative study of evolutionary statistical methods for uncertainty reduction in forest fire propagation prediction. *Procedia Computer Science*, *108*, 2018-2027.

Toledo, G. L., & Ovalle I. I. (1995a) *Medidas de dispersão.* In: Toledo GL & Ovalle II, editors. *Estatística Básica.* 2nd. ed. Atlas S.A. 181–226.

Torres, F. T. P, Roque, M. P. B., Lima, G. S., Martins, S. V., Faria, A. L. L. (2017). Mapeamento do Risco de Incêndios Florestais Utilizando Técnicas de Geoprocessamento. *Floresta e Ambiente*. v. 24.

Toulouse, T., Rossi, L., Celik, T., & Akhloufi, M. (2015). Automatic fire pixel detection using image processing: A comparative analysis of rule-based and machine learning-based methods. *Signal, Image and Video*

Processing., 10(4), 647–654. https://doi.org/10.1007/s11760-015-0789-x.

Veeraswamy, A., Galea, E. R., Filippidis, L., Lawrence, P. J., Haasanen, S., Gazzard, R. J., & Smith, T. E. L. (2018). The simulation of urban-scale evacuation scenarios with application to the Swinley forest fire. *Safety Science., 102*, 178–193.

Wang, S. D., Miao, L. L, Peng, G. X. (2012). An improved algorithm for forest fire detection using HJ data. *Environmental Sciences*, [S.l.], v. 13, 140–150.

Wang, Y., Dang, L., & Ren, J. (2019). Forest fire image recognition based on convolutional neural network. *Journal of Algorithms & Computational Technology., 13*, 174830261988768. https://doi.org/10.1177/1748302619887689.

White, B. L. A., Oliveira, M. V. N., Ribeiro, G. T. (2017). Avaliação e simulação do comportamento do fogo em diferentes fitofisionomias de uma área de mata atlântica do Nordeste Brasileiro. *Floresta*, Curitiba, PR, v. 47, n. 3, p. 247 - 256, jul. / set. 2017.

Zheng, Z. Gao, Y., Yang, Q. et al. (2020). Predicting forest fire risk based on mining rules with ant-miner algorithm in cloud-rich areas. *Ecological Indicators*, 118, 106772 https://doi.org/10.1016/j.ecolind.2020.106772.

Zheng, Z., Huang, W., Li, S., & Zeng, Y. (2016). A new burn severity index based on land surface temperature and enhanced vegetation index. *International Journal of Applied Earth Observation and Geoinformation, 45*, 84–94.

Zheng, Z., Huang, W., Li, S., & Zeng, Y. (2017). Forest fire spread simulating model using cellular automaton with extreme learning machine. *Ecological Modelling, 348*, 33–43.